



Published in final edited form as:

Cell Rep. 2022 December 27; 41(13): 111875. doi:10.1016/j.celrep.2022.111875.

## Mitochondrial genome recovery by ATFS-1 is essential for development after starvation

Nandhitha Uma Naresh<sup>1</sup>, Sookyung Kim<sup>1</sup>, Tomer Shpilka<sup>1</sup>, Qiyuan Yang<sup>1</sup>, Yunguang Du<sup>1</sup>, Cole M. Haynes<sup>1,2,\*</sup>

<sup>1</sup>Department of Molecular, Cell, and Cancer Biology, University of Massachusetts Chan Medical School, Worcester, MA 01605, USA

<sup>2</sup>Lead contact

### SUMMARY

Nutrient availability regulates the *C. elegans* life cycle as well as mitochondrial physiology. Food deprivation significantly reduces mitochondrial genome (mtDNA) numbers and leads to aging-related phenotypes. Here we show that the bZIP (basic leucine zipper) protein ATFS-1, a mediator of the mitochondrial unfolded protein response (UPR<sup>mt</sup>), is required to promote growth and establish a functional germline after prolonged starvation. We find that recovery of mtDNA copy numbers and development after starvation requires mitochondrion-localized ATFS-1 but not its nuclear transcription activity. We also find that the insulin-like receptor DAF-2 functions upstream of ATFS-1 to modulate mtDNA content. We show that reducing DAF-2 activity represses ATFS-1 nuclear function while causing an increase in mtDNA content, partly mediated by mitochondrion-localized ATFS-1. Our data indicate the importance of the UPR<sup>mt</sup> in recovering mitochondrial mass and suggest that *atfs-1*-dependent mtDNA replication precedes mitochondrial network expansion after starvation.

### In brief

Uma Naresh et al. show that the mitochondrial unfolded protein response (UPR<sup>mt</sup>) is required for growth and germline proliferation after prolonged starvation. Mitochondrial localization of the bZIP protein ATFS-1 promotes mtDNA replication and is required to reestablish or regenerate the mitochondrial network depleted by autophagy.

### Graphical Abstract

---

This is an open access article under the CC BY-NC-ND license (<http://creativecommons.org/licenses/by-nc-nd/4.0/>).

\*Correspondence: cole.haynes@umassmed.edu.

#### AUTHOR CONTRIBUTIONS

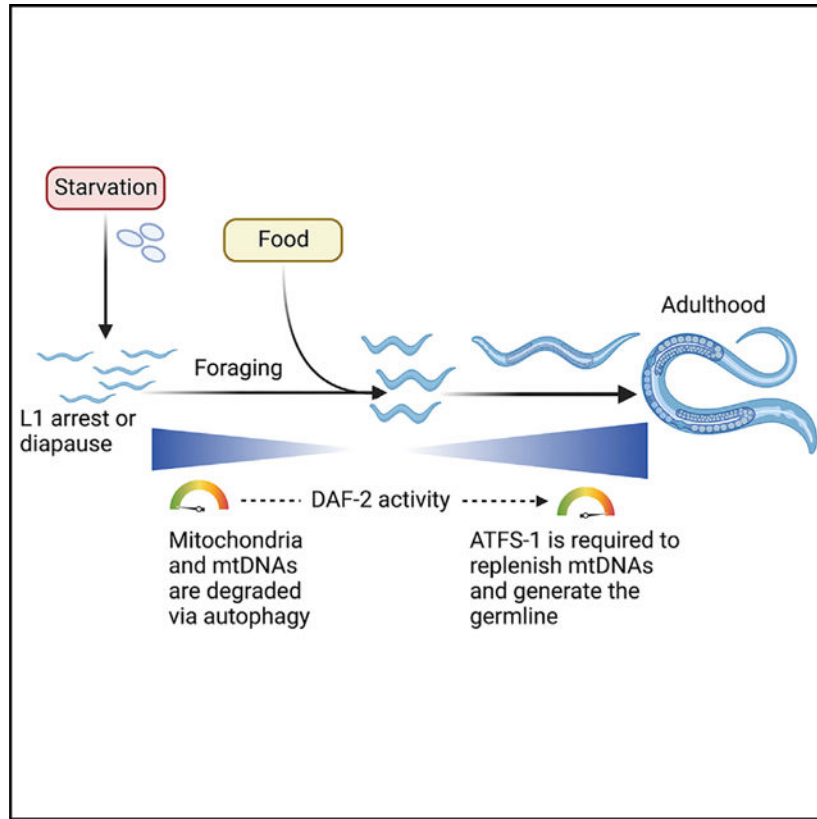
N.U.N., T.S., S.K., and C.M.H. designed the experiments. N.U.N., S.K., Y.D., and Q.Y. generated the worm strains and performed research. N.U.N. and C.M.H. wrote the manuscript.

#### DECLARATION OF INTERESTS

The authors declare no competing interests.

#### SUPPLEMENTAL INFORMATION

Supplemental information can be found online at <https://doi.org/10.1016/j.celrep.2022.111875>.



## INTRODUCTION

The mitochondrial unfolded protein response ( $UPR^{mt}$ ) is a signaling pathway mediated by the bZIP protein ATFS-1 that promotes mitochondrial network expansion by regulating transcription of mitochondrial biogenesis genes.<sup>1</sup> The  $UPR^{mt}$  transcriptional response has been best studied in the context of mitochondrial perturbations that slow worm development, such as mutations in genes encoding oxidative phosphorylation (OXPHOS) proteins, mtDNA heteroplasmy, or pathogen infection.<sup>2–7</sup> During worm development, the majority of ATFS-1 is imported into mitochondria and usually degraded by the protease LONP-1.<sup>8</sup> During mitochondrial stress or dysfunction, a fraction of ATFS-1 accumulates in the nucleus via its nuclear localization sequence (NLS), where it activates a transcription program to recover mitochondrial function.<sup>9</sup> ATFS-1 also accumulates in dysfunctional mitochondria via its mitochondrial targeting sequence (MTS), where it binds mtDNA and promotes replication.<sup>9,10</sup> Regulation of the nuclear transcriptional response as well as mtDNA replication by ATFS-1 during mitochondrial stress is consistent with the  $UPR^{mt}$  promoting mitochondrial function by coordinating mitochondrion-to-nucleus communication (Figure 1A). However, little is known regarding the role of ATFS-1 in coordinating such a response when mitochondrial dysfunction is not induced by exogenous stressors or deleterious mutations.

Diverse species, including vertebrates, adapt cellular responses to survive adverse environmental conditions, including prolonged starvation and extreme seasonal changes

such as drought.<sup>11–14</sup> A relatively common adaptation is when the animals enter a diapause state upon encountering severe stress, where growth is suspended but basal metabolic activities are maintained. The nematode *C. elegans* can undergo developmental arrest during starvation and resume development when food is encountered.<sup>15,16</sup> When worms hatch in the absence of food, they remain arrested at the first larval stage, which is known as L1 diapause. Developmental arrest is accompanied by an increase in stress resistance and alterations in metabolic signaling pathways, including insulin signaling, transforming growth factor  $\beta$  (TGF- $\beta$ ) signaling, AMP-activated protein kinase, and fatty acid metabolism.<sup>17–21</sup> To survive during L1 arrest, energy production requires autophagic degradation of cytosolic components, including organelles such as mitochondria.<sup>21</sup> Sustaining a prolonged search for food during L1 arrest results in manifestation of aging-like phenotypes, including accumulation of protein aggregates and reactive oxygen species as well as fragmentation of the mitochondrial network and depletion of mtDNA.<sup>22,23</sup> When food is encountered, the aging-like deterioration is resolved and growth resumes,<sup>23</sup> accompanied by increased transcription and translation of components required for mitochondrial biogenesis.<sup>24–26</sup>

Nuclear chromosome replication is regulated by numerous proteins and checkpoints to ensure that genome duplication is coordinated with the cell cycle.<sup>27,28</sup> Akin to nuclear genome replication, mtDNA replication is often followed by mitochondrial fission, presumably to ensure that each daughter mitochondrion inherits at least one mtDNA.<sup>29</sup> However, mtDNA replication is not coordinated with the cell cycle. Although the majority of the proteins required for mtDNA replication have been identified, the upstream events that stimulate mtDNA replication remain unclear. Prolonged L1 arrest and the subsequent recovery offers a physiologically relevant as well as genetically tractable model to study the signaling pathways regulating bulk initiation of mtDNA replication and recovery of the mitochondrial network. Here, we examine the role of the UPR<sup>mt</sup> and ATFS-1 in coordinating mtDNA content recovery or expansion after prolonged starvation.

## RESULTS

### ATFS-1 is required for development after prolonged starvation at L1 stage

*atfs-1(null)* worms, which lack the entire open reading frame, have reduced mitochondrial respiration and mitochondrial function at the L4 stage as well a reduction in lifespan (Figure 1B).<sup>1,5</sup> To survive prolonged starvation, mitochondrial function and integrity are required because loss-of-function mutations in the OXPHOS complex III component *isp-1* or in the ubiquinone synthesis component *clk-1* are short lived during L1 arrest.<sup>18</sup> Thus, we hypothesized that ATFS-1 is also required for survival during starvation. *atfs-1(null)* worms survived as long as wild-type worms during L1 arrest (Figure 1C). These data indicate that, despite the reliance on OXPHOS, ATFS-1 is not involved in mitochondrial maintenance or survival during L1 arrest.

We next examined the growth of wild-type and *atfs-1(null)* worms hatched in the presence of food (referred to as “control”) compared with development upon exposure to food after 5 days of L1 arrest (referred to as “L1 arrest-fed”) (Figure 1D). The development of *atfs-1(null)* worms was significantly impaired after L1 arrest (Figures 1E, 1F, and S1A),

whereas wild-type worms developed similarly to worms hatched on food (Figures 1E, 1F, and S1A). When raised in the presence of food, *atfs-1(null)* worms produce progeny, although fecundity is reduced relative to wild-type worms. However, after starvation, *atfs-1(null)* worms did not lay eggs or produce any viable progeny (Figures 1G and S1B). *atfs-1(null)* worms appeared more transparent and were smaller compared with wild-type worms of the same stage, suggestive of abnormal development (Figures S1C and S1D).

Because nearly all *atfs-1(null)* worms were sterile after L1 arrest, we examined the germline using transgenic reporter strains. The GLH-1::GFP fusion protein marks P granules, which are RNA-enriched compartments specific to germ cells.<sup>30</sup> The germlines of *atfs-1(null)* and wild-type worms hatched in the presence of food expressed GLH-1::GFP throughout the germline (Figure 1H). However, *atfs-1(null)* worms that were fed after L1 arrest had only a cluster of germ cells expressing GLH-1::GFP that failed to expand (Figure 1H). We used a reporter strain expressing PIE-1::GFP to examine germline proliferation. Germ cells express PIE-1 to prevent adoption of somatic cell fates by repressing transcription.<sup>31,32</sup> After L1 arrest, the germline in *atfs-1(null)* worms did not proliferate to the point where PIE-1::GFP was expressed (Figure 1I). These data indicate that the ATFS-1 is required to resume growth and establish a functional germline after prolonged L1 arrest.

### ATFS-1 is required for mtDNA content recovery after L1 starvation

Because ATFS-1 promotes mitochondrial maintenance during growth, we examined mitochondrial network morphology using the dye TMRE (tetramethylrhodamine, ethyl ester), which accumulates in functional mitochondria. At the L4 stage, TMRE staining was comparable throughout the soma in wild-type worms fed upon hatching or after 5 days of L1 arrest (Figures 2A and 2B). As expected, *atfs-1(null)* worms accumulated less TMRE than wild-type worms when hatched in the presence of food, as shown previously.<sup>1</sup> However, after 5 days of L1 arrest, TMRE staining was nearly undetectable in *atfs-1(null)* worms compared with worms of similar age hatched on food, indicating that these worms were unable to establish a functional mitochondrial network (Figures 2A and 2B). Because mitochondria were not detectable in *atfs-1(null)* worms with TMRE staining after L1 arrest, we examined mitochondrial content and morphology using a reporter in which the mitochondrial outer membrane translocase TOMM-20 was tagged with mScarlet.<sup>33</sup> We found that, when hatched onto food, mScarlet accumulated along the mitochondrial network in *atfs-1(null)* mutants, similar to wild-type worms (Figure S2A). However, after L1 arrest, *atfs-1(null)* worms had an aberrant network morphology compared with wild-type worms (Figure S2A), suggesting that aspects of mitochondrial biogenesis occur in the absence of *atfs-1*, but the organelles are dysfunctional.

Because *atfs-1(null)* worms harbored dysfunctional mitochondria and were developmentally impaired after prolonged L1 arrest, we hypothesized that worms with impaired OXPHOS dysfunction may also have similar defects when exiting starvation. However, we found that *clk-1(qm30)* and complex II-defective *mev-1(kn-1)* mutant worms developed at the same rate and had similar brood sizes regardless of whether they were hatched in the presence of food or underwent L1 arrest prior to feeding (Figures 2C–2E and S2B–S2D). OXPHOS is reduced in *clk-1(qm30)* and *mev-1(kn-1)* worms but not completely impaired.<sup>34</sup> These data

suggest that the presence of functional ATFS-1 in *clk-1* and *mev-1* mutants allows OXPHOS dysfunction mutants to cope during development after starvation, in contrast to *atfs-1(null)* worms, which lack UPR<sup>mt</sup>-mediated processes.

We have shown previously that, concomitant with reduced membrane potential, *atfs-1(null)* worms harbor fewer mtDNAs than wild-type worms.<sup>1</sup> Thus, we examined the mtDNA content of *atfs-1(null)* worms during L1 arrest and after food introduction. A previous study found that mtDNAs were depleted during L1 arrest by autophagy.<sup>22</sup> Similarly, mtDNA content was reduced by ~50% in wild-type worms after 5 days of L1 arrest (Figure 2F). *atfs-1(null)* worms hatched with similar quantities of mtDNA as wild-type worms, which was also reduced by 50% after 5 days of L1 arrest (Figure 2F). As expected, mtDNA content increased in wild-type worms upon food introduction. However, mtDNA content remained low in *atfs-1(null)* worms (Figure 2G). These data suggest that, when L1 worms begin to feed, ATFS-1 is required to increase or recover the mtDNA content that was degraded during L1 arrest (Figures 2F and 2G).

Wild-type and *atfs-1(null)* worms that are directly hatched onto food contain similar quantities of mtDNA (Figure 2G) and develop into fertile adults, suggesting that *atfs-1* does not regulate mtDNA content in embryos prior to feeding. During starvation, although wild-type and *atfs-1(null)* worms undergo a reduction in mtDNA content, after food introduction, mtDNA increases more slowly in *atfs-1(null)* worms compared with wild-type worms (Figures 2F and 2G). These findings suggest that, for normal development after prolonged L1 arrest, ATFS-1 is required to increase mtDNA content to the level that L1 wild-type and *atfs-1(null)* harbor at the time that they hatch. These findings also emphasize the challenges in mediating the metabolic transition that must occur when the worm goes from a catabolic state to fuel the search for food to an anabolic state required for growth and development when feeding begins.

### **Mitophagy does not impair mtDNA accumulation in *atfs-1(null)* worms after L1 arrest**

Given the reduced mtDNA accumulation in *atfs-1(null)* worms after L1 arrest, we hypothesized that this may be due to impaired mtDNA replication or increased mitophagy-mediated clearance as a result of accumulating mitochondrial damage in the absence of the UPR<sup>mt</sup>. To determine the effect of mitophagy, we examined recovery from L1 arrest in *atfs-1(null);pdr-1(tm598)* worms, which contain a loss-of-function mutation in the ubiquitin ligase Parkin, which is required for mitophagy in *C. elegans*.<sup>6,35</sup> Although *atfs-1(null);pdr-1(tm598)* worms developed slower than either single mutant, they are able to develop to adulthood when hatched in the presence of food without prolonged starvation (Figures S3A and S3B). However, similar to *atfs-1(null)* worms, the development and recovery of mtDNA content after L1 arrest was impaired in *atfs-1(null);pdr-1(tm598)* worms (Figures S3A–S3D). These findings suggest that the impaired recovery of mtDNA content in *atfs-1(null)* worms is not due to mitophagy.

### **ATFS-1-dependent nuclear transcription is not required for mtDNA recovery**

Our findings suggest that recovery of mtDNA content after prolonged L1 arrest could be due to ATFS-1 directly promoting mtDNA replication in mitochondria or regulating

nuclear transcription of genes that promote mtDNA replication. To examine the role of ATFS-1-dependent nuclear transcription, we compared wild-type, *atfs-1(null)*, and mutant worms in which the NLS in ATFS-1 was mutated.<sup>1,10</sup> Consistent with impaired nuclear activity of *atfs-1<sup>NLS</sup>* worms, previous studies have shown that the increase in *atfs-1*-dependent transcription of the nuclear gene *hsp-6* was reduced in *atfs-1<sup>NLS</sup>* worms raised during mitochondrial stress.<sup>1,10</sup> ATFS-1<sup>NLS</sup> is imported into mitochondria and processed similarly to wild-type ATFS-1.<sup>10</sup> *atfs-1<sup>DNLS</sup>* worms had similar lifespans to wild-type worms, whereas the lifespan of *atfs-1(null)* worms was considerably reduced (Figure 1B). We generated *clk-1(qm30);atfs-1<sup>DNLS</sup>* worms to examine the effect of reduced *atfs-1*-dependent nuclear transcription during mitochondrial dysfunction. We found that *clk-1(qm30);atfs-1<sup>NLS</sup>* worms developed considerably more slowly and produced fewer progeny than *clk-1(qm30)* worms, indicating that the nuclear activity of ATFS-1 is required for growth during OXPHOS perturbation (Figures S4A and S4B).

We next examined the role of ATFS-1 nuclear activity during development after prolonged L1 arrest. *atfs-1<sup>NLS</sup>* worms developed much faster than *atfs-1(null)* worms (Figures 3A–3C). Upon feeding after prolonged L1 arrest, mtDNA content increased at similar rates in wild-type and *atfs-1<sup>NLS</sup>* worms but was impaired in *atfs-1(null)* worms (Figures 3D and 3E). Unlike *atfs-1(null)* worms, *atfs-1<sup>NLS</sup>* worms established a functional mitochondrial network upon feeding, as determined by TMRE staining (Figures 2A and 2B). However, the mitochondrial network was more fragmented in *atfs-1<sup>NLS</sup>* worms relative to wild-type worms (Figure S4C), indicating that *atfs-1-dependent* transcription is required to maintain optimal mitochondrial function after prolonged starvation.

To examine the role of mitochondrion-localized ATFS-1 in recovery from L1 arrest, we evaluated the mitochondrial network in *atfs-1<sup>R/R</sup>* worms in which the strength of the ATFS-1 MTS was increased by substituting the threonine and aspartic acid residues at positions 10 and 24 with arginine residues. Consistent with increased import of ATFS-1<sup>R/R</sup> into mitochondria, *atfs-1<sup>R/R</sup>* worms have an impaired nuclear response during mitochondrial stress and a fragmented mitochondrial network, as shown previously.<sup>1</sup> Similar to *atfs-1<sup>NLS</sup>* worms, L1 arrested *atfs-1<sup>R/R</sup>* worms developed to adulthood upon feeding (Figure S4D). The mtDNA content in *atfs-1<sup>R/R</sup>* worms was also higher than in *atfs-1(null)* worms exiting prolonged L1 arrest (Figure S4E). These findings indicate that mitochondrion-localized ATFS-1 is required to resume growth and recover mtDNA content after prolonged L1 arrest.

We found previously that ATFS-1 binds directly to mtDNA in dysfunctional mitochondria and that inhibition of *atfs-1* during mitochondrial stress results in an aberrant increase of mtDNA-encoded OXPHOS transcripts.<sup>9</sup> We hypothesized that, in addition to promoting mtDNA recovery, mitochondrion-localized ATFS-1 might also limit mtDNA-encoded transcript accumulation to promote development after starvation. We found that several mtDNA-encoded mRNAs were increased in *atfs-1(null)* worms but not nuclear genome-encoded OXPHOS genes after introduction of food after starvation (Figures S4F and S4G). These findings suggest that, in addition to promoting mtDNA replication, mitochondrion-localized ATFS-1 represses or limits transcription of mtDNA-encoded OXPHOS transcripts during growth upon feeding after prolonged L1 starvation, potentially to facilitate efficient OXPHOS complex assembly.<sup>9</sup>

We next sought to determine whether the *atfs-1-mediated* recovery of mtDNA content is required for recovery from prolonged L1 arrest. Thus, we exposed L1-arrested wild-type worms to ethidium bromide (EtBr), which intercalates in mtDNA and inhibits replication<sup>2,36</sup> and transcription.<sup>37</sup> Exposure to 10 or 30 mg/mL EtBr modestly affected development of wild-type worms hatched directly onto food (Figures 3F and 3G). The same doses severely impaired development of worms after prolonged L1 arrest (Figures 3F and 3H). These data suggest that recovery of mtDNA copy numbers mediated by mitochondrion-localized ATFS-1 is required for growth and germline development after prolonged L1 arrest, but it is difficult to determine the effect of aberrant mtDNA transcription.

### ***daf-2* inhibition promotes *atfs-1*-dependent mtDNA replication**

Last, we sought to gain insight into the upstream events regulating *atfs-1*-dependent mtDNA replication that occur after prolonged L1 arrest. We and others found previously that inhibition of the insulin-like receptor DAF-2 using a hypomorphic mutant (*daf-2(e1370)*) impairs *atfs-1*-dependent induction of *hsp-6<sub>pr</sub>::gfp* during mitochondrial stress (Figure 4A), suggesting that DAF-2 activity promotes nuclear accumulation of ATFS-1.<sup>1,38</sup> *daf-2(e1370)* worms hatched in the presence of food harbored nearly 1.5-fold more mtDNAs than wild-type worms at the L4 stage, suggesting that modest inhibition of DAF-2 promotes mtDNA replication<sup>39</sup> (Figure 4B). We found that the increase in mtDNAs was abrogated in *daf-2(e1370);atfs-1(null)* mutants (Figure 4B). *daf-2(e1370);atfs-1<sup>NLS</sup>* worms harbored similar amounts of mtDNAs as *daf-2(e1370)* worms (Figure 4C), suggesting that mitochondrion-localized ATFS-1 promotes mtDNA replication when *daf-2* is inhibited. Consistent with ATFS-1 localizing to mitochondria, a chromatin precipitation (ChIP) assay using ATFS-1-specific antibodies<sup>9</sup> indicated that ATFS-1 interacts with 2-fold more mtDNAs upon DAF-2 inhibition (Figure 4D). These data indicate that decreased DAF-2 activity reduces *atfs-1*-dependent transcription in the nucleus and allows mitochondrion-localized ATFS-1 to increase mtDNA content.

Next we examined the effect of L1 arrest on the mtDNA content of *daf-2(e1370)* mutants. Although *daf-2(e1370)* worms hatched with increased mtDNA content relative to wild-type worms, mtDNA content declined at similar rates in both strains during L1 arrest (Figure S5A). We hypothesized that the increased mtDNA content in *daf-2(e1370)* worms throughout L1 arrest can be advantageous for growth or recovery after prolonged L1 arrest. As expected, growth and mtDNA levels were impaired in wild-type worms exposed to EtBr, whereas *daf-2(e1370)* worms developed to adulthood and had increased mtDNA content after prolonged L1 arrest (Figures S5B–S5D), suggesting that the lack of mtDNA is a rate-limiting factor for growth after starvation.

We next examined the role of ATFS-1 in recovery of *daf-2(e1370)* worms after prolonged starvation. *daf-2(e1370);atfs-1(null)* worms did not develop into mature adults (Figure 4E). However, *daf-2(e1370);atfs-1<sup>NLS</sup>* worms developed into fertile adults, similar to wild-type worms (Figure 4E). *daf-2(e1370);atfs-1(null)* worms harbor fewer mtDNAs relative to *daf-2(e1370)* and *daf-2(e1370);atfs-1<sup>NLS</sup>* worms after starvation, suggesting that ATFS-1 functions downstream of DAF-2 inhibition to increase the mtDNA content (Figures 4F and 4G) required for development after prolonged L1 arrest. However, it remains unclear

why *daf-2(e1370);atfs-1(null)* worms fail to develop after prolonged L1 arrest because they harbor similar quantities of mtDNA as wild-type and *atfs-1<sup>NLS</sup>* worms, which recover efficiently from L1 arrest.

The FOXO-like transcription factor DAF-16 is the canonical downstream effector activated upon DAF-2 inhibition. DAF-16 promotes L1 survival by regulating transcription of numerous genes, including the cyclin-dependent kinase inhibitor, and by altering metabolic flux to promote trehalose synthesis during L1 arrest.<sup>20,40</sup> *daf-16* loss-of-function mutant worms are unable to develop after prolonged L1 arrest.<sup>41</sup> *daf-2(e1370);daf-16(mu86)* worms had fewer mtDNAs than *daf-2(e1370)* worms, consistent with DAF-16 also promoting mtDNA accumulation when *daf-2* is inhibited (Figure S5E). Thus, we sought to understand the relationship between *daf-16* and *atfs-1*, using the partial deletion mutant *daf-16(mu86).daf-2(e1370);daf16(mu86);atfs-1(null)* worms had a slight but not significant reduction in mtDNAs compared with either single deletion, suggesting that both ATFS-1 and DAF-16 function downstream of DAF-2 to regulate mtDNA content. However, it remains unclear whether ATFS-1 and DAF-16 function in parallel pathways or in the same pathway (Figure S5F). Because *daf-16*-mutants are unable to maintain and survive prolonged L1 arrest,<sup>20,40</sup> the role of DAF-16 in increasing mtDNA content upon feeding remains unclear. Based on these data, we conclude that a reduction in DAF-2 activity leads to increased mtDNA content, partially dependent on mitochondrial ATFS-1, which promotes growth and mitochondrial recovery after prolonged starvation.

## DISCUSSION

*C. elegans* mature from egg to reproductive adult within 3 days. However, during development, worms can enter a diapause-like state at different developmental stages to endure prolonged stress, including starvation.<sup>42</sup> Worms that hatch in the absence of food remain developmentally arrested at the L1 stage and can survive for over 30 days (Figure 1C).<sup>23</sup> To sustain the search for food, cytosolic components, including mitochondria, are degraded by autophagy, which is used to generate ATP via OX-PHOS.<sup>21,22</sup> When food is encountered, a major challenge to resumption of development is repairing the cellular and tissue damage incurred in the absence of food.<sup>23</sup>

Here, we find that, after 5 days of L1 arrest, ATFS-1 is required for development and to establish a functional germline. A previous study found a strong correlation between mutations that extend L1 survival and mutations that extend the adult lifespan.<sup>43</sup> In contrast, we found that, although *atfs-1(null)* worms are relatively short-lived when hatched in presence of food, the absence of ATFS-1 does not affect L1 survival. ATFS-1 does not appear to have any role in the mtDNA accumulation that occurs during embryogenesis through the L1 stage. During prolonged L1 arrest, mtDNAs, and presumably whole mitochondria, are degraded via autophagy.<sup>22</sup> Our findings indicate that mtDNA depletion via autophagy occurs independent of ATFS-1 during L1 arrest. However, to mature into reproductive adults after introduction of food, ATFS-1 is essential to increase or recover the mtDNA content depleted during L1 arrest to a level comparable with that of newly hatched worms. The NLS in ATFS-1 required for *atfs-1*-dependent nuclear transcription was not required to recover mtDNA content or establish a functional mitochondrial network or

functional germline. However, *atfs-1<sup>NLS</sup>* worms have perturbed mitochondrial morphology at the L4 stage, consistent with ATFS-1 coordinating mitochondrial network expansion with the increased levels of protein synthesis and growth that occur upon feeding.<sup>1</sup>

Lastly, our findings suggest that the activity of mitochondrion-localized ATFS-1 is required to increase mtDNA content upon inhibition of the insulin receptor-like protein DAF-2. We found previously that *daf-2*-inhibition impairs *atfs-1*-dependent transcription, potentially by impairing S6 kinase and reducing general rates of protein synthesis, which result in the majority of ATFS-1 trafficking to mitochondria.<sup>1</sup> Here, we find that a reduction in DAF-2 function causes an increase in mtDNA content, which requires ATFS-1, but not ATFS-1-dependent, nuclear transcription, suggesting that a reduction in DAF-2 activity promotes mtDNA replication via mitochondrion-localized ATFS-1. We propose that this “toggle switch”-like activity of DAF-2 ensures that synthesis of mtDNAs occurs prior to activation of the transcription program required for expansion of the mitochondrial network driven by TORC1-dependent protein synthesis during worm development. These findings are consistent with our previous work indicating that mitochondrion-localized ATFS-1 promotes mtDNA replication in dysfunctional mitochondria, which can contribute to a replicative advantage of deleterious mtDNAs in a disease model.<sup>6,10</sup> Our finding that ATFS-1 is required to increase mtDNA replication and recover mtDNAs degraded during starvation suggest a reason why such a pathway may have evolved because recovery of mtDNA content after L1 arrest is essential for development and *C. elegans* reproduction.

### Limitations of the study

In the current study, we demonstrated a requirement for ATFS-1 in worm development after prolonged L1 arrest. Our findings suggest that ATFS-1 is required to recover the mtDNA content depleted during L1 arrest because of autophagy. To examine mitochondrial function, we utilized the functional dye TMRE and mScarlet fused to TOMM-20, which accumulates on the mitochondrial membrane independent of mitochondrial function. These tools enable assessment of mitochondrial function and morphology. However, we did not perform higher-resolution imaging such as electron microscopy, which may provide further insight into the mitochondrial defects that occur in the absence of ATFS-1 after L1 arrest. We found that the development of wild-type worms after L1 arrest was impaired by exposure to EtBr, whereas worms that hatched in the presence of food developed relatively normally with low EtBr concentrations. Because EtBr is a known inhibitor of mtDNA replication,<sup>44</sup> we interpreted these findings to suggest that mtDNA replication is essential for recovery from prolonged L1 arrest. However, because ATFS-1 is also a negative regulator of transcription of mtDNA-encoded genes, we cannot rule out a role of aberrant transcription in impaired recovery from L1 arrest. Lastly, we suggest a role of DAF-2 in regulating the ATFS-1-dependent increase in mtDNA content after L1 arrest. The increased mtDNA content in *daf-2(e1270)* worms relative to wild-type worms partially requires ATFS-1, and the development of *daf-2(e1270)* worms after L1 arrest also requires ATFS-1. However, *daf-2(e1270);atfs-1(null)* worms have similar levels of mtDNA as *atfs-1<sup>NLS</sup>* worms, which are able to develop after L1 arrest. The underlying biology remains unclear but may involve other downstream regulators of DAF-2. Because metabolism and growth are considerably altered in *daf-2(e1270)* worms, their reliance on mitochondrial function and mtDNA for development may also be altered.

## STAR★METHODS

### RESOURCE AVAILABILITY

**Lead contact**—Further information and requests for reagents or strains must be directed to and will be fulfilled by the lead contact, Cole Haynes (cole.haynes@umassmed.edu).

**Materials availability**—This study did not generate new unique materials.

#### Data and code availability

- All data reported in this paper will be shared by the lead contact upon request.
- This paper does not report original code.
- Any additional information required to reanalyze the data deposited in this paper is available from the lead contact upon request.

### EXPERIMENTAL MODEL AND SUBJECT DETAILS

**C. elegans strains**—*C. elegans* strains were fed and cultured on HT115 Escherichia Coli strain at 20°C unless otherwise specified. The reporter strain *hsp-6<sub>pr</sub>::gfp* was used for visualizing UPR<sup>mt</sup> activation.<sup>2</sup> N2 (wildtype), *clk-1(qm30)*, *daf-2(e1370)*, *daf-16(mu86)* strains were obtained from the CGC. PIE:GFP and GLH-1:GFP were gifts from Dr. Craig Mello. *pdr-1(tm598)* was obtained from the National BioResource project (Tokyo, Japan). *atfs-1(null)*, *atfs-1<sup>NLS</sup>*, and the *atfs-1<sup>R/R</sup>* strains were generated using CRISPR-Cas9 as described.<sup>1,5,10</sup> *vha-6p:tomm-20(1–54):mScarlet* strain was a gift from Dr. Gary Ruvkun 33.

### METHOD DETAILS

**Starvation plates and recovery from prolonged L1 arrest**—For L1 arrest, worms were synchronized by bleaching and transferred to NGM plates that lacked cholesterol and peptone for 5 days.<sup>46</sup> Following L1 arrest, the worms were transferred to NGM plates seeded with HT115 bacteria (L1 arrest-fed condition). Control condition worms were synchronized by bleaching and allowed to hatch directly on NGM plates seeded with HT115 bacteria. All strains were maintained at 20°C throughout all experiments. For images of worm development, the L1 arrest-fed worms of each strain were compared to control worms of the same developmental stage.

**Brood size quantification**—Three L4 stage nematodes were randomly selected from each condition and transferred to a fresh plate and incubated at 20°C. Once worms reached adulthood, the number of progenies were quantified until the worms stopped laying eggs. Brood size was determined as the average number of progenies per worm on each plate based on the sum of total eggs. Five biological replicates per strain per condition were used and 10–15 worms were used for quantification of eggs from each replicate.

**mtDNA quantification**—mtDNA was measured using quantitative PCR (qPCR) similar to previously published methods.<sup>1,6,47</sup> 30–40 worms were collected per sample in lysis buffer containing 50 mM KCl, 10 mM Tris-HCl pH 8.3, 2.5 mM MgCl<sub>2</sub>, 0.45% NP-40, 0.45% Tween 20, 0.01% gelatin, fresh stock of 200 mg/mL proteinase K) and immediately frozen

at  $-80^{\circ}\text{C}$  for at least 15 min followed by lysis at  $65^{\circ}\text{C}$  for 80 min.  $2\mu\text{L}$  of lysate was used per reaction, and they were performed in biological and technical triplicates using iQ SYBR Green Supermix and the Biorad qPCR CFX96 (Bio-Rad Laboratories). The average  $C_t$  (threshold cycle) of technical replicate values were obtained for mtDNA and was normalized using the  $2^{-C_t}$  method. Primers that specifically amplify mtDNA are listed in Table S2. Primers that amplify a non-coding region near the nuclear-encoded *ges-1* gene were used as a control. Student's *t*-test or one-way ANOVA was used to determine the statistical significance where applicable.

For measuring mtDNA recovery in Figure 2H over time course of 24 h, control worms were synchronized to L1s overnight prior to transferring on bacteria seeded plates and L1 arrest-fed worms were starved for 5 days prior to transferring on bacteria seeded plates.

**RNA isolation and qRT-PCR**—Worms were harvested from plates into tubes and washed 3 times using *S. basal* to remove bacteria. 1 mL of TRIzol Reagent (Invitrogen) was added to the worm pellet and the tubes were flash frozen using liquid nitrogen. Total RNA was isolated from worm pellets using the TRIzol Reagent and chloroform. cDNA was then synthesized from total RNA using the iScript cDNA Synthesis Kit (Bio-Rad). qPCR was performed using iQ SYBR Green Supermix. Primer sequences are listed in Table S2. Relative expression of target genes was normalized to the house keeping gene *act-3*. Fold changes in gene expression were calculated.

For qPCR of L1 worms, liquid cultures of different worm strains were grown for at least two generations with food and then prepped for eggs using bleach solution to obtain synchronized L1s. For L1 arrest-fed condition, eggs were hatched onto starvation plates for 5 days and then fed up to L2s before harvesting for RNA extraction. For control condition, eggs directly hatched on food were grown up to L2s were collected and used for RNA extraction.

**Body length measurements**—Body length quantifications were obtained at the L4 stage. However, as the *clk-1(qm30)* and *clk-1(qm30); atfs-1<sup>NLS</sup>* strains developed slowly, body length measurements were obtained on day 1 of egg lay. Body length measurements were obtained using ImageJ measuring from nose tip to worm tail as previously described.<sup>48</sup>

**Microscopy**—*C. elegans* were imaged using either a Zeiss AxioCam 506 mono camera mounted on a Zeiss Axio Imager Z2 microscope, a Zeiss AxioCam MRc camera mounted on a Zeiss SteREO Discovery V12 stereoscope or a ZEISS LSM800 confocal microscope. Exposure times were the same for each sample in each experiment.

**L1 starvation survival**—L1 survival assay was adapted from protocol previously described.<sup>18</sup> Worms were grown for at least two generations at  $20^{\circ}\text{C}$  in liquid with food and bleached to collect eggs, which hatched overnight on a shaker incubator in S-basal without cholesterol. Synchronized L1s were maintained in 25- or 125-mL flasks at a concentration of  $\sim 1$  worm/ml in 10–12 mL of S-basal without cholesterol and without antibiotics. Flasks were shaken at 200 rpm in a shaker at  $20^{\circ}\text{C}$  except when scoring. Viability was assessed by aliquoting 100 to 200  $\mu\text{L}$  of worms to fresh plates and monitoring the number of worms

that were alive or dead after 2 days post plating. The worms were scored every other day and the survival percent was calculated based on a ratio of the number of worms survived to total number of plated worms on each scoring day. The graph shows data collected from one biological replicate representative of 3 independent replicates. Summary statistics of 3 independent biological replicates are reported in Table S1. Lifespan variability between experiments may be due to variation in population density between biological replicates.<sup>49</sup>

**Adult lifespan assay**—Animals were raised on seeded NGM plates at 20°C until the L4 stage and ~100 L4 worms were transferred to fresh bacterial plates (10 worms per plate). Worms were scored every 2–3 days and those that were unresponsive to touch of the worm pick were marked as dead. Worms that bagged or crawled off the plate were censored and not included in the study. The figure shows data collected from a single experiment. Each experiment was repeated in 3 independent biological replicates (Table S3).

**DAPI staining**—Animals were grown on control or L1 arrest-fed condition until day 1 adulthood. Then, the worms were washed off the plates and placed in microcentrifuge tube containing 0.01% Tween-PBS. Worms were pelleted by low-speed centrifugation and washed 2–3 times with 0.01% Tween PBS. Next, 1 mL of pre-chilled methanol from –20°C was added to the whole worm pellet and tubes were immediately placed in the freezer at –20°C for exactly 5 min. The worms were pellet again and rinsed 2–3 times with 0.1% Tween-PBS. 0.2 µL of DAPI solution was added and the tube was allowed in sit in the dark for 5 min and after, rinsed with 0.1% Tween-PBS. Finally, 30 µL of 75% glycerol solution was added to worm pellet and were ready to be imaged.

**TMRE staining**—Freshly seeded HT115 bacterial plates were coated with TMRE to make a final concentration of 30 µm in each plate. The worms were either synchronized by bleaching and plated onto TMRE plates either from egg stage (control) or starved in L1 stage for 5 days using starvation plates and then transferred to TMRE plates (L1 arrest-fed). Three independent biological repeats were performed. The graph was generated by quantifying of 15–25 individual worms from a single experimental repeat that is representative of all three biological replicates. TMRE quantification was done as previously described.<sup>1</sup> In brief, the average pixel intensity values were calculated by sampling images of different worms. The average pixel intensity for each animal was calculated using ImageJ (<http://rsb.info.nih.gov/ij/>). Mean values were compared using two-way ANOVA.

**Mitochondrial morphology quantification**—For morphology analysis, 3–4 worms were placed on a fresh 4% agarose pad on a single slide and scored within 5 min by imaging using a ZEISS LSM800 confocal microscope (minimal time was spent for each slide as prolonged exposure may induce network fission). All visible cells in each worm were scored on based 3 levels of classification as tubular, intermediate and fragmented as previously described.<sup>23</sup> Three biological replicates were analyzed with ~10–15 worms scored in each replicate.

**Ethidium bromide experiments**—Control worms were bleached directly onto plates containing 0, 10 or 30 mg/mL ethidium bromide with HT115 bacteria. For starved-fed condition, worms were first bleached onto starvation plates for 5 days and then transferred

onto ethidium bromide plates as described above. Plates were imaged when at the L4 stage or when they became developmentally arrested.

**ChIP-mtDNA**—ATFS-1 ChIP was performed as previously described.<sup>10</sup> Synchronized worms were cultured on plates and harvested at the L4 stage. The worms were lysed via Teflon homogenizer in chilled PBS with protease inhibitors (Roche). Cross-linking of DNA and protein was performed by treating worms with 1.85% formaldehyde containing protease inhibitors for 15 min. Glycine was added to a final concentration of 125 mM and incubated for 5 min at room temperature to quench the formaldehyde. The tubes were cold centrifuged at 3000 rpm for 2 min and then, pellets were resuspended twice in cold PBS with protease inhibitors. Samples were treated with lysis buffer containing 0.1% Sarkosyl, protease inhibitors in FA Buffer (50 mM HEPES/KOH pH 7.5, 1mM EDTA, 1% Triton X-100, 0.1% Sodium deoxycholate, 150 mM NaCl). The supernatant was precleaned with pre-blocked ChIP-grade Pierce magnetic protein A/G beads (Thermo Scientific) and then incubated with Monoclonal Mouse mAb IgG1 Isotype Control (Cell Signaling Technology, G3A1) rotating overnight at 4C. The antibody-DNA complex was precipitated with protein A/G magnetic beads or protein A Sepharose beads (Invitrogen). After washing, the crosslinks were reversed by incubation at 65°C overnight. The samples were then treated with RNaseA at 37°C for 1.5 h followed by proteinase K treatment at 55°C for 2 h. Lastly, the immunoprecipitated and input DNA were purified with ChIP DNA Clean & Concentrator (Zymo Research, D5205) and used as templates for qPCR.

## QUANTIFICATION AND STATISTICAL ANALYSIS

All experiments were performed at least three times and all the represented graphs are based on biologically independent replicates. “n” represents number of biological replicates in figure legends. L1 starvation survival and adult life span are graphs from a single biological replicate representative of three independent biological repeats. The summary statistics from three biological replicates are reported in Tables S1 and S3. For lifespan analysis, statistics were performed using OASIS2 software<sup>45</sup> and values were calculated with the log rank/Mantel Cox test. p values were calculated by the two-tailed Student’s t-test, one-way ANOVA or two-way ANOVA with post-hoc analyses. The statistical tests were chosen based on previous studies with similar methodologies and analysis performed using Graphpad Prism 7. Experiments were not blinded, and randomization was not used. For all figures, the mean  $\pm$  SD is represented unless otherwise noted.

## Supplementary Material

Refer to Web version on PubMed Central for supplementary material.

## ACKNOWLEDGMENTS

We thank the Caenorhabditis Genetics Center for providing *C. elegans* strains, funded by NIH Office of Research 362 Infrastructure Programs (P40 OD010440). This work was supported by HHMI and National Institutes of Health grants (R37AG047182-08 and R56AG075204) to C.M.H.

## INCLUSION AND DIVERSITY

We support inclusive, diverse, and equitable conduct of research.

## REFERENCES

1. Shpilka T, Du Y, Yang Q, Melber A, Uma Naresh N, Lavelle J, Kim S, Liu P, Weidberg H, Li R, et al. (2021). UPR(mt) scales mitochondrial network expansion with protein synthesis via mitochondrial import in *Caenorhabditis elegans*. *Nat. Commun* 12, 479. 10.1038/s41467-020-20784-y. [PubMed: 33473112]
2. Yoneda T, Benedetti C, Urano F, Clark SG, Harding HP, and Ron D. (2004). Compartment-specific perturbation of protein handling activates genes encoding mitochondrial chaperones. *J. Cell Sci* 117, 4055–4066. 10.1242/jcs.01275. [PubMed: 15280428]
3. Durieux J, Wolff S, and Dillin A. (2011). The cell-non-autonomous nature of electron transport chain-mediated longevity. *Cell* 144, 79–91. 10.1016/j.cell.2010.12.016. [PubMed: 21215371]
4. Moullan N, Mouchiroud L, Wang X, Ryu D, Williams EG, Mottis A, Jovaisaite V, Frochaux MV, Quiros PM, Deplancke B, et al. (2015). Tetracyclines disturb mitochondrial function across eukaryotic models: a call for caution in biomedical research. *Cell Rep.* 10, 1681–1691. 10.1016/j.celrep.2015.02.034. [PubMed: 25772356]
5. Deng P, Uma Naresh N, Du Y, Lamech LT, Yu J, Zhu LJ, Pukkila-Worley R, and Haynes CM (2019). Mitochondrial UPR repression during *Pseudomonas aeruginosa* infection requires the bZIP protein ZIP-3. *Proc. Natl. Acad. Sci. USA* 116, 6146–6151. 10.1073/pnas.1817259116. [PubMed: 30850535]
6. Lin YF, Schulz AM, Pellegrino MW, Lu Y, Shaham S, and Haynes CM (2016). Maintenance and propagation of a deleterious mitochondrial genome by the mitochondrial unfolded protein response. *Nature* 533, 416–419. 10.1038/nature17989. [PubMed: 27135930]
7. Gitschlag BL, Kirby CS, Samuels DC, Gangula RD, Mallal SA, and Patel MR (2016). Homeostatic responses regulate selfish mitochondrial genome dynamics in *C. elegans*. *Cell Metab.* 24, 91–103. 10.1016/j.cmet.2016.06.008. [PubMed: 27411011]
8. Nargund AM, Pellegrino MW, Fiorese CJ, Baker BM, and Haynes CM (2012). Mitochondrial import efficiency of ATFS-1 regulates mitochondrial UPR activation. *Science* 337, 587–590. 10.1126/science.1223560. [PubMed: 22700657]
9. Nargund AM, Fiorese CJ, Pellegrino MW, Deng P, and Haynes CM (2015). Mitochondrial and nuclear accumulation of the transcription factor ATFS-1 promotes OXPHOS recovery during the UPR(mt). *Mol. Cell* 58, 123–133. 10.1016/j.molcel.2015.02.008. [PubMed: 25773600]
10. Yang Q, Liu P, Anderson NS, Shpilka T, Du Y, Naresh NU, Li R, Zhu LJ, Luk K, Lavelle J, et al. (2022). LONP-1 and ATFS-1 sustain deleterious heteroplasmy by promoting mtDNA replication in dysfunctional mitochondria. *Nat. Cell Biol* 24, 181–193. 10.1038/s41556-021-00840-5. [PubMed: 35165413]
11. Hu CK, Wang W, Brind'Amour J, Singh PP, Reeves GA, Lorincz MC, Alvarado AS, and Brunet A. (2020). Vertebrate diapause preserves organisms long term through Polycomb complex members. *Science* 367, 870–874. 10.1126/science.aaw2601. [PubMed: 32079766]
12. Van Gilst M. (2020). A time to grow and a time to pause. *Science* 367, 851–852. 10.1126/science.aba8064. [PubMed: 32079759]
13. Hu CK, and Brunet A. (2018). The African turquoise killifish: a research organism to study vertebrate aging and diapause. *Aging Cell* 17, e12757. 10.1111/ace1.12757.
14. Hand SC, Denlinger DL, Podrabsky JE, and Roy R. (2016). Mechanisms of animal diapause: recent developments from nematodes, crustaceans, insects, and fish. *Am. J. Physiol. Regul. Integr. Comp. Physiol* 310, R1193–R1211. 10.1152/ajpregu.00250.2015. [PubMed: 27053646]
15. Baugh LR (2013). To grow or not to grow: nutritional control of development during *Caenorhabditis elegans* L1 arrest. *Genetics* 194, 539–555. 10.1534/genetics.113.150847. [PubMed: 23824969]

16. Carranza-García E, and Navarro RE (2020). Insights into the hypometabolic stage caused by prolonged starvation in L4-adult *Caenorhabditis elegans* hermaphrodites. *Front. Cell Dev. Biol* 8, 124. 10.3389/fcell.2020.00124. [PubMed: 32211406]
17. Kaplan REW, Chen Y, Moore BT, Jordan JM, Maxwell CS, Schindler AJ, and Baugh LR (2015). *dbl-1/TGF-beta* and *daf-12/NHR* signaling mediate cell-nonautonomous effects of *daf-16/FOXO* on starvation-induced developmental arrest. *PLoS Genet.* 11, e1005731. 10.1371/journal.pgen.1005731.
18. Lee BH, and Ashrafi K. (2008). A TRPV channel modulates *C. elegans* neurosecretion, larval starvation survival, and adult lifespan. *PLoS Genet.* 4, e1000213. 10.1371/journal.pgen.1000213.
19. Demoinet E, Li S, and Roy R. (2017). AMPK blocks starvation-inducible transgenerational defects in *Caenorhabditis elegans*. *Proc. Natl. Acad. Sci. USA* 114, E2689–E2698. 10.1073/pnas.1616171114. [PubMed: 28289190]
20. Baugh LR, and Sternberg PW (2006). *DAF-16/FOXO* regulates transcription of *cki-1/Cip/Kip* and repression of *lin-4* during *C. elegans* L1 arrest. *Curr. Biol* 16, 780–785. 10.1016/j.cub.2006.03.021. [PubMed: 16631585]
21. Kang C, You YJ, and Avery L. (2007). Dual roles of autophagy in the survival of *Caenorhabditis elegans* during starvation. *Genes Dev.* 21, 2161–2171. 10.1101/gad.1573107. [PubMed: 17785524]
22. Hibshman JD, Leuthner TC, Shoben C, Mello DF, Sherwood DR, Meyer JN, and Baugh LR (2018). Nonselective autophagy reduces mitochondrial content during starvation in *Caenorhabditis elegans*. *Am. J. Physiol. Cell Physiol* 315, C781–C792. 10.1152/ajpcell.00109.2018. [PubMed: 30133321]
23. Roux AE, Langhans K, Huynh W, and Kenyon C. (2016). Reversible-age-related phenotypes induced during larval Quiescence in *C. elegans*. *Cell Metab.* 23, 1113–1126. 10.1016/j.cmet.2016.05.024. [PubMed: 27304510]
24. Baugh LR, Demodena J, and Sternberg PW (2009). RNA Pol II accumulates at promoters of growth genes during developmental arrest. *Science* 324, 92–94. 10.1126/science.1169628. [PubMed: 19251593]
25. Wang J, and Kim SK (2003). Global analysis of dauer gene expression in *Caenorhabditis elegans*. *Development* 130, 1621–1634. 10.1242/dev.00363. [PubMed: 12620986]
26. Stadler M, and Fire A. (2013). Conserved translational remodeling in nematode species executing a shared developmental transition. *PLoS Genet.* 9, e1003739. 10.1371/journal.pgen.1003739.
27. Vermeulen K, Van Bockstaele DR, and Berneman ZN (2003). The cell cycle: a review of regulation, deregulation and therapeutic targets in cancer. *Cell Prolif* 36, 131–149. 10.1046/j.1365-2184.2003.00266.x. [PubMed: 12814430]
28. Sclafani RA, and Holzen TM (2007). Cell cycle regulation of DNA replication. *Annu. Rev. Genet* 41, 237–280. 10.1146/annurev.genet.41.110306.130308. [PubMed: 17630848]
29. Lewis SC, Uchiyama LF, and Nunnari J. (2016). ER-mitochondria contacts couple mtDNA synthesis with mitochondrial division in human cells. *Science* 353, aaf5549. 10.1126/science.aaf5549.
30. Seydoux G. (2018). The P granules of *C. elegans*: a genetic model for the study of RNA-protein condensates. *J. Mol. Biol* 430, 4702–4710. 10.1016/j.jmb.2018.08.007. [PubMed: 30096346]
31. Mello CC, Schubert C, Draper B, Zhang W, Lobel R, and Priess JR (1996). The PIE-1 protein and germline specification in *C. elegans* embryos. *Nature* 382, 710–712. 10.1038/382710a0. [PubMed: 8751440]
32. Reese KJ, Dunn MA, Waddle JA, and Seydoux G. (2000). Asymmetric segregation of PIE-1 in *C. elegans* is mediated by two complementary mechanisms that act through separate PIE-1 protein domains. *Mol. Cell* 6, 445–455. 10.1016/s1097-2765(00)00043-5. [PubMed: 10983990]
33. Mao K, Ji F, Breen P, Sewell A, Han M, Sadreyev R, and Ruvkun G (2019). Mitochondrial dysfunction in *C. elegans* activates mitochondrial relocalization and nuclear hormone receptor-dependent detoxification genes. *Cell Metab.* 29, 1182–1191.e4. 10.1016/j.cmet.2019.01.022. [PubMed: 30799287]
34. Felkai S, Ewbank JJ, Lemieux J, Labbé JC, Brown GG, and Hekimi S. (1999). CLK-1 controls respiration, behavior and aging in the nematode *Caenorhabditis elegans*. *EMBO J.* 18, 1783–1792. 10.1093/emboj/18.7.1783. [PubMed: 10202142]

35. Narendra D, Tanaka A, Suen DF, and Youle RJ (2008). Parkin is recruited selectively to impaired mitochondria and promotes their autophagy. *J. Cell Biol* 183, 795–803. 10.1083/jcb.200809125. [PubMed: 19029340]
36. Martinus RD, Garth GP, Webster TL, Cartwright P, Naylor DJ, Høj PB, and Hoogenraad NJ (1996). Selective induction of mitochondrial chaperones in response to loss of the mitochondrial genome. *Eur. J. Biochem* 240, 98–103. 10.1111/j.1432-1033.1996.0098h.x. [PubMed: 8797841]
37. Zylber E, Vesco C, and Penman S. (1969). Selective inhibition of the synthesis of mitochondria-associated RNA by ethidium bromide. *J. Mol. Biol* 44, 195–204. 10.1016/0022-2836(69)90414-8. [PubMed: 5811827]
38. Gatsi R, Schulze B, Rodríguez-Palero MJ, Hernando-Rodríguez B, Baumeister R, and Artal-Sanz M. (2014). Prohibitin-mediated lifespan and mitochondrial stress implicate SGK-1, insulin/IGF and mTORC2 in *C. elegans*. *PLoS One* 9, e107671. 10.1371/journal.pone.0107671.
39. Haroon S, Li A, Weinert JL, Fritsch C, Ericson NG, Alexander-Floyd J, Braeckman BP, Haynes CM, Bielas JH, Gidalevitz T, and Vermulst M. (2018). Multiple molecular mechanisms rescue mtDNA disease in *C. elegans*. *Cell Rep.* 22, 3115–3125. 10.1016/j.celrep.2018.02.099. [PubMed: 29562168]
40. Hibshman JD, Doan AE, Moore BT, Kaplan RE, Hung A, Webster AK, Bhatt DP, Chitrakar R, Hirschey MD, and Baugh LR (2017). *daf-16/FoxO* promotes gluconeogenesis and trehalose synthesis during starvation to support survival. *Elife* 6, e30057. 10.7554/eLife.30057.
41. Olmedo M, Mata-Cabana A, Rodríguez-Palero MJ, García-Sánchez S, Fernández-Yanez A, Merrow M, et al. (2020). Prolonged quiescence delays somatic stem cell-like divisions in *Caenorhabditis elegans* and is controlled by insulin signaling. *Aging Cell* 19, e13085. 10.1111/ace1.13085.
42. Baugh LR, and Hu PJ (2020). Starvation responses throughout the *Caenorhabditis elegans* life cycle. *Genetics* 216, 837–878. 10.1534/genetics.120.303565. [PubMed: 33268389]
43. Muñoz MJ, and Riddle DL (2003). Positive selection of *Caenorhabditis elegans* mutants with increased stress resistance and longevity. *Genetics* 163, 171–180. 10.1093/genetics/163.1.171. [PubMed: 12586705]
44. Tsang WY, and Lemire BD (2002). Mitochondrial genome content is regulated during nematode development. *Biochem. Biophys. Res. Commun* 291, 8–16. 10.1006/bbrc.2002.6394. [PubMed: 11829454]
45. Han SK, Lee D, Lee H, Kim D, Son HG, Yang JS, Lee SJV, and Kim S. (2016). Oasis 2: online application for survival analysis 2 with features for the analysis of maximal lifespan and healthspan in aging research. *Oncotarget* 7, 56147–56152. 10.18632/oncotarget.11269. [PubMed: 27528229]
46. Stiernagle T. (2006). Maintenance of *C. elegans* (WormBook), pp. 1–11. 10.1895/wormbook.1.101.1.
47. Valenci I, Yonai L, Bar-Yaacov D, Mishmar D, and Ben-Zvi A. (2015). Parkin modulates heteroplasmy of truncated mtDNA in *Caenorhabditis elegans*. *Mitochondrion* 20, 64–70. 10.1016/j.mito.2014.11.001. [PubMed: 25462019]
48. Mörck C, and Pilon M. (2006). *C. elegans* feeding defective mutants have shorter body lengths and increased autophagy. *BMC Dev. Biol* 6, 39. 10.1186/1471-213X-6-39. [PubMed: 16884547]
49. Artyukhin AB, Schroeder FC, and Avery L. (2013). Density dependence in *Caenorhabditis* larval starvation. *Sci. Rep* 3, 2777. 10.1038/srep02777. [PubMed: 24071624]

### Highlights

- The mitochondrial UPR is required for *C. elegans* growth after prolonged starvation
- UPR<sup>mt</sup> is required to increase mtDNA replication after starvation-induced mtDNA decline
- Mitochondrial localization of the bZIP protein ATFS-1 promotes mtDNA content recovery
- The insulin-like receptor DAF-2 coordinates ATFS-1-mediated mtDNA replication and growth

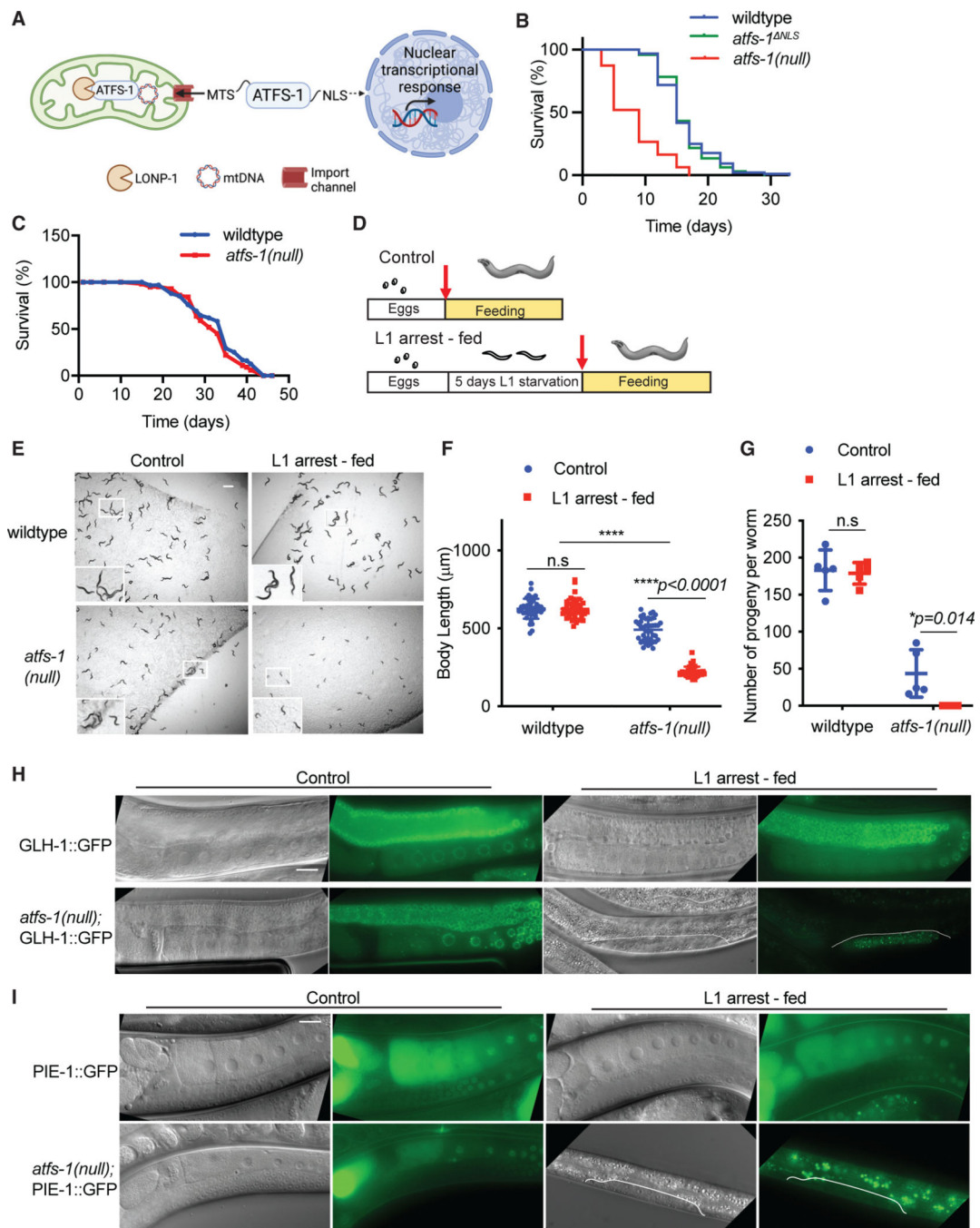


**Figure 1. ATFS-1 is required for development after prolonged L1 arrest**

(A) Schematic illustrating ATFS-1-mediated UPR<sup>mt</sup> signaling.

(B) Lifespan analysis comparing wild-type, *atfs-1*(null), and *atfs-1*<sup>NLS</sup> worms (statistical analyses from three independent repeats are reported in Table S3).

(C) Lifespan analysis comparing wild-type and *atfs-1*(null) worms during L1 arrest (statistical analyses from three independent repeats are reported in Table S1).

(D) Schematic depicting the experimental protocol comparing worms that were directly hatched in the presence of bacteria (control) and worms that were maintained as arrested L1s for 5 days and then transferred to plates seeded with bacteria (L1 arrestfed).

(E) Images of wild-type and *atfs-1(null)* worms under control and L1 arrest-fed conditions, obtained when control worms reached the L4 stage (scale bar, 0.5 mm).

(F) Quantification of body length, comparing wild-type and *atfs-1(null)* worms under control and L1 arrest-fed conditions ( $n = 3 \pm \text{SD}$ , \*\*\*\* $p < 0.0001$ , two-way ANOVA with post-hoc Sidak's test).

(G) Brood size quantification of wild-type and *atfs-1(null)* worms under control and L1 arrest-fed conditions ( $n = 5 \pm \text{SD}$ , \* $p = 0.014$ , two-way ANOVA with post-hoc Sidak's test).

(H) Images of wild-type and *atfs-1(null)* worms expressing GLH-1::GFP under control or L1 arrest-fed conditions, obtained when the control worms reached day 1 of adulthood (scale bar, 0.02 mm).

(I) Images of wild-type and *atfs-1(null)* worms expressing PIE-1::GFP under control or L1 arrest-fed conditions obtained when the control worms reached day 1 of adulthood (scale bar, 0.02 mm).

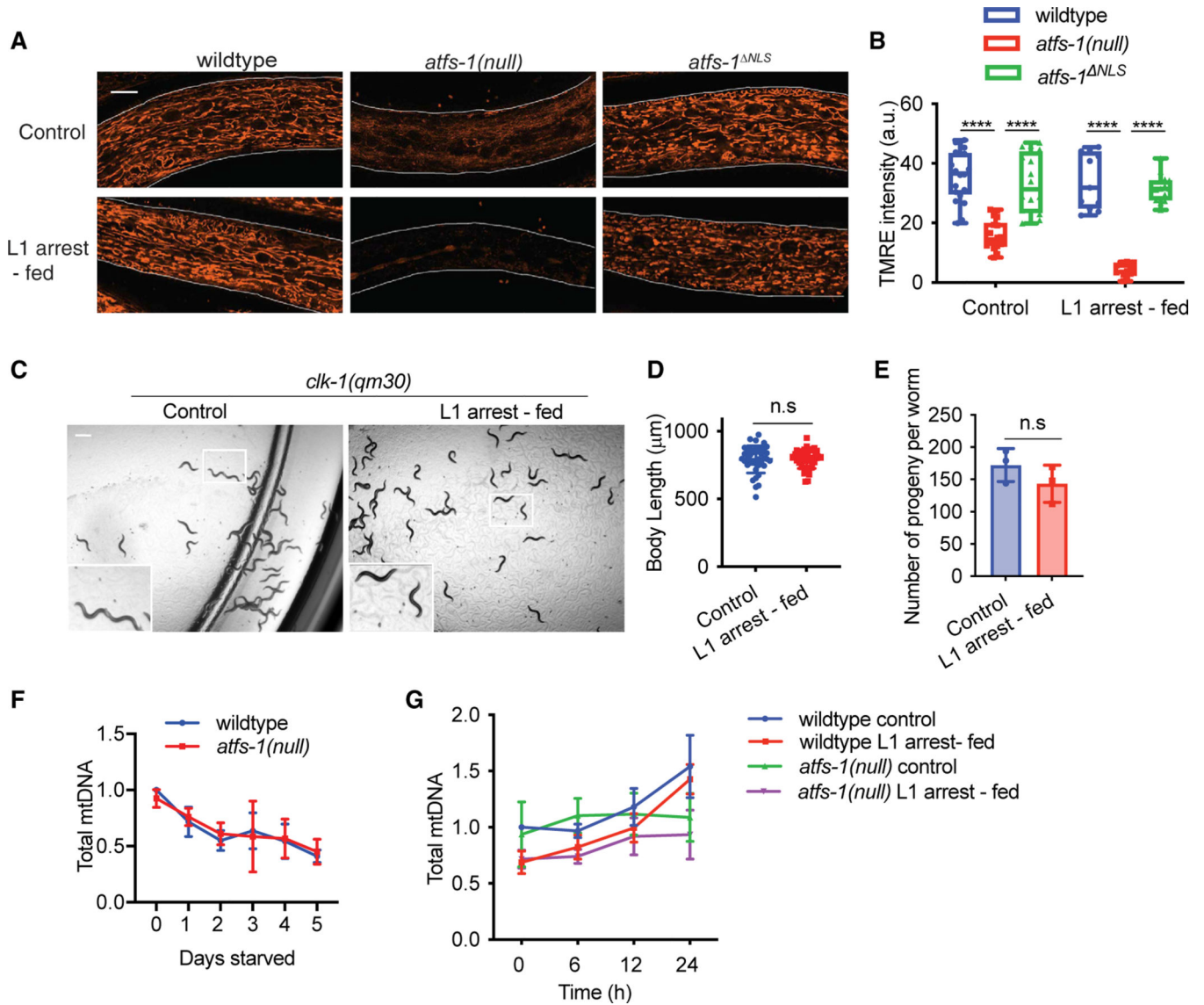


**Figure 2. UPR<sup>mt</sup> promotes mtDNA content recovery after starvation**

(A) Images comparing TMRE staining of wild-type, *atfs-1(null)*, and *atfs-1<sup>NLS</sup>* worms under control or L1 arrest-fed conditions, obtained when control worms reached the L4 stage (scale bar, 10 μm; representative images from three biological replicates).

(B) Quantification of TMRE staining of wild-type, *atfs-1(null)*, and *atfs-1<sup>NLS</sup>* worms at the L4 stage under control or L1 arrest-fed conditions (n = 15–20 worms for each strain and condition ± SD, \*\*\*\*p < 0.0001, two-way ANOVA with post-hoc Sidak’s test; a.u., arbitrary unit).

(C) Images comparing development of *clk-1(qm30)* worms under control and L1 arrest-fed conditions on day 1 of adulthood (scale bar, 0.5 mm).

(D) Body length quantification of *clk-1(qm30)* worms under control and L1 arrest-fed conditions, measured on day 1 of adulthood (n = 3 ± SD, Student’s t test).

(E) Brood size quantification of *clk-1(qm30)* worms under control and L1 arrest-fed conditions (n = 3 ± SD, 10–15 worms each replicate, Student’s t test).

(F) mtDNA quantification of wild-type and *atfs-1(null)* starved L1 worms over a period of 5 days as determined by qPCR ( $n = 3 \pm SD$ , one-way ANOVA; wild-type worms: \*\*\* $p = 0.0007$ , post hoc Dunnett's test shows significant difference between 0-day starved worms and 1- to 5-day starved worms; *atfs-1(null)* worms: \* $p = 0.0191$ , post-hoc Dunnett's test shows significant difference between 0-day starved worms and 3- to 5-day starved worms). (G) Time course of mtDNA content quantification over 24 h as determined by qPCR comparing wild-type and *atfs-1(null)* worms under control and L1 arrest-fed conditions ( $n = 6$  for wild-type and  $n = 3$  for *atfs-1(null)*  $\pm SD$ , \*\* $p = 0.0039$  comparing L1 arrest-fed wild-type and *atfs-1(null)* mtDNA content after 24 h of feeding, two-way ANOVA with post hoc Tukey's multiple comparisons test).

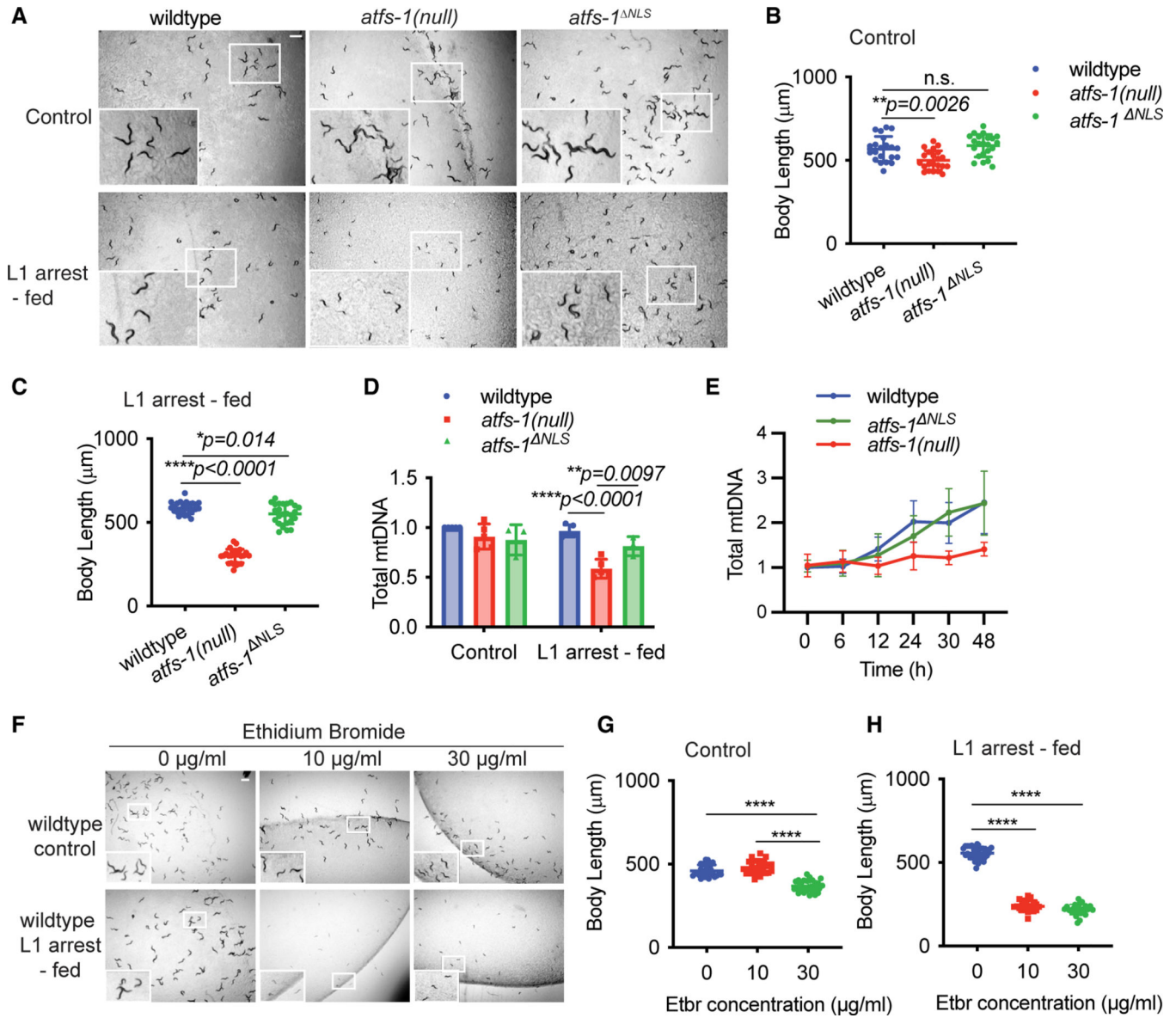


**Figure 3. The increase in mtDNA content after L1 arrest does not require *atfs-1*-dependent nuclear transcription**

(A) Images of wild-type, *atfs-1(null)*, and *atfs-1<sup>NLS</sup>* worms under control and L1 arrest-fed conditions, obtained when the control condition worms reached the L4 stage (scale bar, 0.5 mm).

(B) Quantification of body length of wild-type, *atfs-1(null)*, and *atfs-1<sup>NLS</sup>* worms under control conditions when the worms reached the L4 stage ( $n = 3 \pm SD$ ,  $**p = 0.0026$ , one-way ANOVA with post hoc Dunnett’s test).

(C) Quantification of body length of wild-type, *atfs-1(null)*, and *atfs-1<sup>NLS</sup>* worms under L1 arrest-fed conditions when the control worms reached the L4 stage ( $n = 3 \pm SD$ ,  $*p = 0.014$  comparing wild-type and *atfs-1<sup>NLS</sup>* worms and  $****p < 0.0001$  comparing wild-type and *atfs-1(null)* worms, one-way ANOVA with post hoc Dunnett’s test).

(D) mtDNA quantification of wild-type, *atfs-1(null)*, and *atfs-1<sup>NLS</sup>* worms when the control condition worms reached the L4 stage ( $n = 3-5 \pm SD$ , \*\*\*\* $p < 0.0001$  comparing wild-type and *atfs-1(null)* worms and \*\* $p = 0.0097$  comparing *atfs-1(null)* and *atfs-1<sup>NLS</sup>* L1 arrest-fed worms, two-way ANOVA with post hoc Tukey's multiple comparisons test).

(E) Time course of mtDNA quantification by qPCR comparing wild-type, *atfs-1(null)*, and *atfs-1<sup>NLS</sup>* worms fed for 48 h after L1 arrest ( $n = 4 \pm SD$  for wild-type \* $p = 0.029$  comparing wild-type and *atfs-1(null)* worm mtDNA at 48 h, \* $p = 0.035$  comparing *atfs-1(null)* and *atfs-1<sup>NLS</sup>* worm mtDNA at 48 h, two-way ANOVA with post hoc Tukey's multiple comparisons test).

(F) Images of wild-type control and L1 arrest-fed worms treated with 0, 10, and 30  $\mu\text{g/mL}$  of EtBr when the control worms reached the L4 stage (scale bar, 0.5 mm).

(G) Quantification of body length of wild-type control worms treated with 0, 10, and 30  $\mu\text{g/mL}$  of EtBr, measured when worms treated with 0  $\mu\text{g/mL}$  EtBr reached the L4 stage ( $n = 3$ , \*\*\*\* $p < 0.0001$ , one-way ANOVA with post hoc Tukey's test).

(H) Quantification of body length of wild-type L1 arrest-fed worms treated with 0, 10, and 30  $\mu\text{g/mL}$  of EtBr when the worms treated with 0  $\mu\text{g/mL}$  EtBr reached the L4 stage ( $n = 3$ , \*\*\*\* $p < 0.0001$ , one-way ANOVA with post hoc Tukey's test).

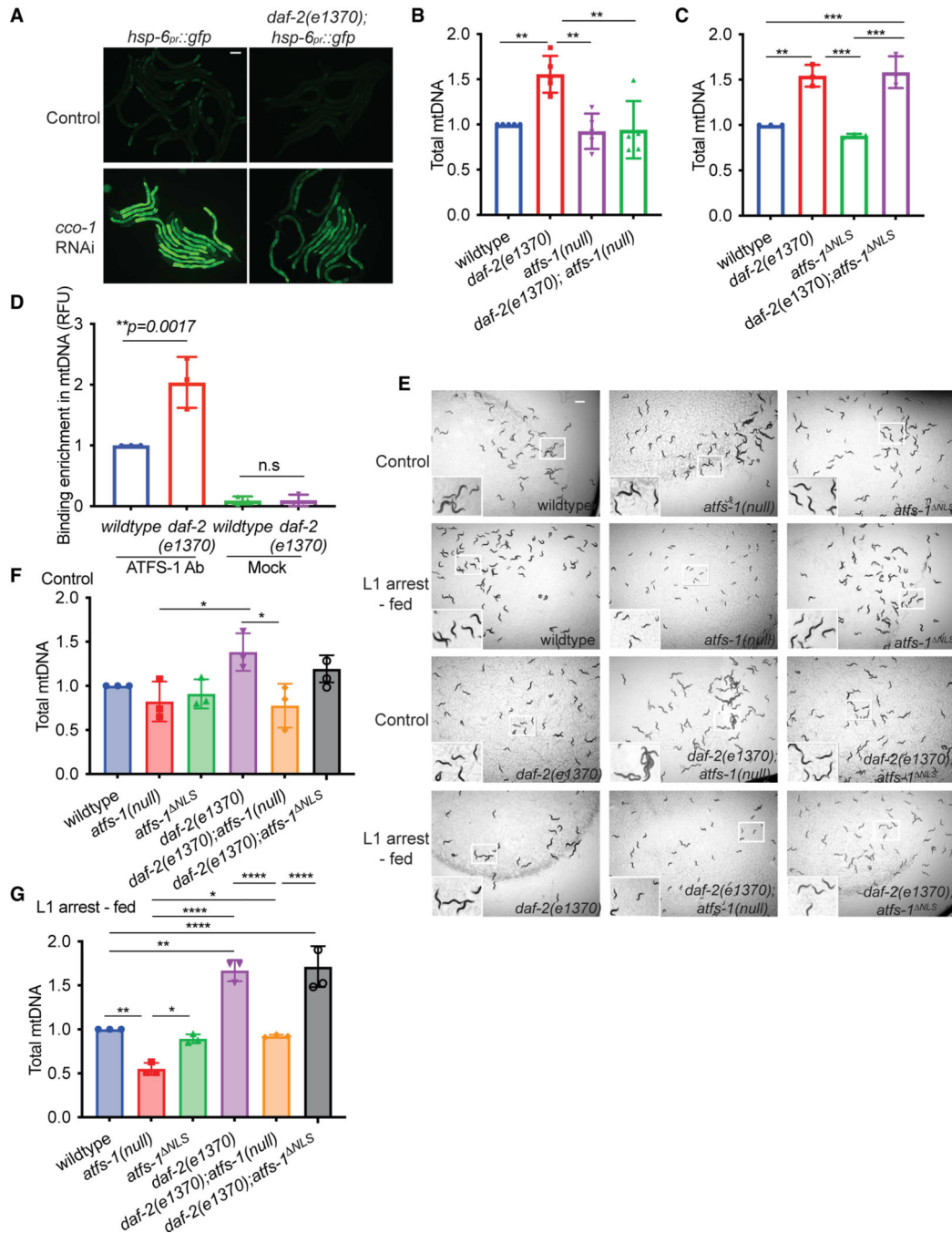


**Figure 4. *daf-2* inhibition promotes *atfs-1*-dependent mtDNA replication**

(A) Fluorescence images of *hsp-6<sub>pr</sub>::gfp* and *daf-2(e1370);hsp-6<sub>pr</sub>::gfp* worms raised on control or *cco-1(RNAi)* at the L4 stage (scale bar, 0.1 mm).

(B) mtDNA quantification of wild-type, *atfs-1(null)*, *daf-2(e1370)*, and *daf-2(e1370);atfs-1(null)* worms, determined at the L4 stage (n = 5 ± SD, \*\*\*\**p* < 0.0001, one way ANOVA with post hoc Tukey’s multiple comparisons test).

- (C) mtDNA quantification of wild-type, *atfs-1<sup>NLS</sup>*, *daf-2(e1370)*, and *daf-2(e1370);atfs-1<sup>DNLS</sup>* worms determined at the L4 stage ( $n = 3 \pm \text{SD}$ , \*\*\*\* $p < 0.0001$ , one-way ANOVA with post hoc Tukey's multiple comparison test).
- (D) mtDNA quantification after ATFS-1 or control CHIP in wild-type and *daf-2(e1370)* worms at the L4 stage ( $n = 3 \pm \text{SD}$ , \*\* $p = 0.0017$ , one-way ANOVA with post hoc Tukey's multiple comparisons test).
- (E) Images of wild-type, *atfs-1(null)*, *atfs-1<sup>NLS</sup>*, *daf-2(e1370)*, *daf-2(e1370);atfs-1(null)*, and *daf-2(e1370);atfs-1<sup>NLS</sup>* worms under control and L1 arrest-fed conditions, obtained when control worms reached the L4 stage (scale bar, 0.5 mm).
- (F) mtDNA quantification of wild-type, *atfs-1(null)*, *atfs-1<sup>NLS</sup>*, *daf-2(e1370)*, *daf-2(e1370);atfs-1(null)*, and *daf-2(e1370);atfs-1<sup>NLS</sup>* worms under control conditions, as determined by qPCR at the L4 stage ( $n = 3 \pm \text{SD}$ , \* $p = 0.132$ , one-way ANOVA with post hoc Tukey's multiple comparisons test).
- (G) mtDNA quantification of wild-type, *atfs-1(null)*, *atfs-1<sup>NLS</sup>*, *daf-2(e1370)*, *daf-2(e1370);atfs-1(null)*, and *daf-2(e1370);atfs-1<sup>NLS</sup>* worms under L1 arrest conditions, as determined by qPCR when control worms reached the L4 stage ( $n = 3 \pm \text{SD}$ , \*\*\*\* $p < 0.0001$ , one-way ANOVA with post hoc Tukey's multiple comparisons test).

## KEY RESOURCES TABLE

| REAGENT or RESOURCE                                   | SOURCE   | IDENTIFIER  |
|---|--|---|
| Chemicals, peptides, and recombinant proteins         |  |   |
| Ethidium Bromide                                      | Invitrogen   | 15585011  |
| TMRE  | Thermo Fisher  | T669  |
| Experimental models: Organisms/strains                |  |   |
| <i>C. elegans</i> : MQ130 ( <i>clk-1(qm30)</i> )      | Caenorhabditis Genetics Center (CGC)                               | RRID: WB Cat#: WBStrain00026639   |
| <i>C. elegans</i> : CB1370 ( <i>daf-2(e1370)</i> )    | Caenorhabditis Genetics Center (CGC)                               | RRID: WB Cat#: WBStrain00004309   |
| <i>C. elegans</i> : CB1038 ( <i>daf-16(mu86)</i> )    | Caenorhabditis Genetics Center (CGC)                               | RRID: WB Cat#: WBStrain00004840   |
| <i>atfs-1<sup>NLS</sup></i>                           | Shpilka et al., 2021, <sup>1</sup> Yang et al., 2022 <sup>10</sup> | N/A   |
| <i>atfs-1<sup>R/R</sup></i>                           | Shpilka et al., 2021 <sup>1</sup>                                  | N/A   |
| <i>pdr-1(tm598)</i>                                   | National BioResource Project (Tokyo, Japan)                        | N/A   |
| <i>atfs-1(null)</i>                                   | Deng et al., 2019 <sup>5</sup>                                     | N/A   |
| PIE-1::GFP  | Laboratory of Dr. Craig C. Mello                                   | N/A   |
| GLH-1::GFP  | Laboratory of Dr. Craig C. Mello                                   | N/A   |
| <i>vha-6p::tomm-20(1–54)::mScarlet</i>                | Laboratory of Dr. Gary Ruvkun                                      | N/A   |
| Oligonucleotides                                      |  |   |
| Full list of qRT-PCR primers is presented in Table S2 | This paper   | N/A   |
| Software and algorithms                               |  |   |
| Fiji ImageJ   | ImageJ   | RRID:SCR_002285   |
| Prism   | Graphpad   | RRID:SCR_002798   |
| OASIS2  | Han et al., 2016 <sup>45</sup>                                     | <a href="https://sbi.postech.ac.kr/oasis2/surv/">https://sbi.postech.ac.kr/oasis2/surv/</a> |
| Biorender   | Biorender  | <a href="https://biorender.com/">https://biorender.com/</a>                                 |